

Supporting Information

A Nonsymmetric Dy₂ Single-Molecule Magnet with two Relaxation Processes Triggered by External Magnetic Field: Theoretical and Integrated EPR study of the Role of Magnetic-Site Dilution

Nikolia Lalioti,[†] Vassilis Nastopoulos,[†] Nikos Panagiotou,[‡] Anastasios Tasiopoulos,[‡] Nikolaos

Ioannidis,^{||*} Joris van Slageren,^{∞*} Peng Zang,^{⊗,∞} Gopalan Rajaraman,^{##} Abinash Swain,[#] and Vassilis Tangoulis^{†*}

[†] Department of Chemistry, Laboratory of Inorganic Chemistry, University of Patras, 26504 Patras, Greece

[‡] Department of Chemistry, University of Cyprus, 1678 Nicosia, Cyprus

^{||} Institute of Nanoscience and Nanotechnology, NCSR “Demokritos”, 153 10 Aghia Paraskevi Attikis, Greece

[⊗] School of Chemistry & Chemical Engineering, Shaanxi Normal University Xi'an, 710199, China

[∞] Institut für Physikalische Chemie, Universität Stuttgart, Pfaffenwaldring 55, D-70569 Stuttgart, Germany

[#] Department of Chemistry, Indian Institute of Technology Bombay, Powai, Mumbai - 400 076, India

Tables

Table S1. Crystal data and structure refinement for 1·MeOH at 106.8(2) and Dy@Y2 at 107.7(6) K.....	4
Table S2. Coordination geometry analysis for the 8-coordinated metal atoms Dy1 and Dy2 of 1·MeOH by the SHAPE v2.1 software.	5
Table S3. Selected Bond lengths [Å] for 1·MeOH at 106.8(2) K with estimated standard deviations in parentheses.....	6
Table S4. Bond angles [°] for 1·MeOH at 106.8(2) K with estimated standard deviations in parentheses.....	7
Table S5. Geometry (Å, °) of the strong hydrogen-bonding motifs in compound 1·MeOH	9
Table S6. Bond lengths [Å] for Y@Dy2 at 107.7(6) K with estimated standard deviations in parentheses.....	9
Table S7. Selected Bond angles [°] for Dy@Y2 at 107.7(6) K with estimated standard deviations in parentheses.....	10
Table S8. Parameters obtained by fitting the Cole-Cole plots (1500 dc field, Figure 4e) of 1·MeOH using the sum of two generalized Debye functions.....	16
Table S9. Parameters obtained by fitting the out-of-phase (Figure 5b) versus T ac magnetic susceptibility signals for Dy@Y2 in a 3.0 G ac field oscillating between 1488 and 10 Hz using the sum of two generalized Debye functions.	17
Table S10. Ab Initio CASSCF/RASSI-SO calculations of the energy barrier of the lowest 8 KD of both Dy centers in 1·MeOH along with the deviation in the angle of the excited state anisotropic axis with respect to the ground state.....	18
Table S11. Ab initio computed crystal field parameters for Dy-1 and Dy-2 centres of 1·MeOH	19

Figures

Figure S 1. The IR spectra (KBr, cm^{-1}) of 1·MeOH and Dy@Y2	20
Figure S 2. Experimental and theoretical X-ray powder patterns of 1·MeOH and Dy@Y2	21
Figure S 3. Partially labelled plot of the crystal structure of Dy@Y2 . The polyhedral representations of the Y^{III} atoms are also shown. Hydrogen atoms and the dopant Dy^{III} ions have been omitted for the shake of clarity.....	22
Figure S 4. (upper) Dc magnetic susceptibility of of 1·MeOH and Dy@Y2 in the 300-2 K temperature range under an applied field of 0.1 T. (lower) Isothermal magnetization curves of 1·MeOH and Dy@Y2 at 2K and 5K.	23
Figure S 5. <i>Field dependence of the out-of-phase ac susceptibility signals for 1·MeOH</i>	24
Figure S 6. (a)-(b) The weak temperature dependent χ'' signals were observed under zero dc field, indicating a small effective barrier. (c)-(d) No linear region is observed in Arrhenius fitting, while an exponential (T^n) fitting gives n value close to 1, suggesting the direct relaxation process present here. (e) The fitting of Cole-Cole plots with a generalized Debye model gives α values between 0.12 and 0.34. All curves are refer to 1·MeOH	25
Figure S 7. Under zero field, no χ_M'' peaks were observed for the sample Dy@Y2	26
Figure S 8. LoProp charge on the surrounding O of both Dy-1 and Dy-2 centres of 1·MeOH .26	
Figure S 9. Poly_aniso fitted magnetic susceptibility for sample 1·MeOH (solid spheres). The magnetic susceptibility of Dy@Y2 (solid triangles) is also presented for comparison reasons	27
Figure S 10. Spin density plots for the high spin and broken symmetry states, obtained from the density function calculations using broken symmetry approach for 1·MeOH	28

Table S1. Crystal data and structure refinement for **1**•MeOH at 106.8(2) and **Dy@Y2** at 107.7(6) K.

Empirical formula	C ₇₄ H ₆₂ Dy ₂ O ₁₄	C ₇₄ H ₆₂ Dy _{0.14} O ₁₄ Y _{1.86}
Formula weight	1500.23	1363.18
Temperature	106.8(2) K	107.7(6) K
Wavelength	1.54184 Å	1.54184 Å
Crystal system	Triclinic	Triclinic
Space group	P $\bar{1}$	P $\bar{1}$
Unit cell dimensions	a = 11.2128(4) Å b = 16.0056(7) Å c = 18.6715(9) Å α = 78.035(4)° β = 75.762(4)° γ = 72.617(4)°	a = 11.1868(4) Å b = 16.0404(6) Å c = 18.6620(6) Å α = 78.186(3)° β = 75.862(3)° γ = 72.605(3)°
Volume	3067.0(2) Å ³	3067.2(2) Å ³
Z	2	2
Density (calculated)	1.624 g/cm ³	1.476 g/cm ³
Absorption coefficient	13.456 mm ⁻¹	3.813 mm ⁻¹
F(000)	1500	1399
Crystal size	0.09 x 0.06 x 0.05 mm	0.05x 0.03 x 0.03 mm
θ range for data collection	3.54 to 73.17°	3.54 to 73.55°
Index ranges	-8<=h<=13, -17<=k<=19, -22<=l<=22	-13<=h<=11, -19<=k<=19, -22<=l<=20
Reflections collected	20441	20366
Independent reflections	11046 [R _{int} = 0.0322]	11053 [R _{int} = 0.0391]
θ /completeness	67.5°/99.9%	67.5°/99.9%
Refinement method	Full-matrix least-squares on F ²	Full-matrix least-squares on F ²
Data / restraints / parameters	11046 / 44 / 825	11053 / 50 / 827
Goodness-of-fit on F ²	1.037	1.019
Final R indices [I > 2 σ (I)]	R ₁ = 0.0382, wR ₂ = 0.0969	R ₁ = 0.044, wR ₂ = 0.113
R indices [all data]	R ₁ = 0.0454, wR ₂ = 0.1022	R ₁ = 0.056, wR ₂ = 0.123
Largest diff. peak and hole	1.892 and -0.670 e·Å ⁻³	1.673 and -0.703 e·Å ⁻³

$R_1 = \sum ||F_o| - |F_c|| / \sum |F_o|$, $wR_2 = \{\sum [w(F_o^2 - F_c^2)^2] / \sum [w(F_o^2)^2]\}^{1/2}$ and $w = 1 / [\sigma^2(F_o^2) + (aP)^2 + bP]$ where $P = (F_o^2 + 2F_c^2) / 3$ and a and b are the two weighting parameters suggested by the SHELXL refinement software.

Table S2. Coordination geometry analysis for the 8-coordinated metal atoms Dy1 and Dy2 of 1·MeOH by the SHAPE v2.1 software.

	CShM value		Symmetry	Polyhedron
	Dy1	Dy2		
1·MeOH				
	28.802	28.284	D_{8h}	Octagon
	23.095	22.121	C_{7v}	Heptagonal pyramid
	15.634	16.787	D_{6h}	Hexagonal bipyramid
	9.179	9.596	O_h	Cube
	0.607	0.494	D_{4d}	Square antiprism
	1.959	1.781	D_{2d}	Triangular dodecahedron
	14.268	15.472	D_{2d}	Johnson gyrobifastigium J26
	27.337	27.330	D_{3h}	Johnson elongated triangular bipyramid J14
	2.502	2.535	C_{2v}	Biaugmented trigonal prism J50
	1.894	1.788	C_{2v}	Biaugmented trigonal prism
	4.921	4.484	D_{2d}	Snub diphenooid J84
	9.808	10.354	T_d	Triakis tetrahedron
	22.661	22.574	D_{3h}	Elongated trigonal bipyramid

Table S3. Selected Bond lengths [Å] for **1**·MeOH at 106.8(2) K with estimated standard deviations in parentheses.

Distance	Value
O1-DY2	2.342(3)
O1-DY1	2.360(3)
O1M-DY2	2.383(3)
O2-DY1	2.428(3)
O2M-H2M	0.852(10)
O3-DY1	2.302(3)
O4-DY1	2.362(3)
O5-DY1	2.255(3)
O6-DY1	2.336(3)
O7-DY1	2.365(3)
O7-DY2	2.376(3)
O8-DY2	2.402(3)
O9-DY2	2.360(3)
O10-DY2	2.337(3)
O10-DY1	2.403(3)
O11-DY2	2.266(3)
O12-DY2	2.289(3)
DY1-DY2	3.5669(3)

Table S4. Bond angles [°] for 1·MeOH at 106.8(2) K with estimated standard deviations in parentheses.

Angle	Value
DY2-O1-DY1	98.69(10)
DY1-O7-DY2	97.57(10)
DY2-O10-DY1	97.63(10)
O5-DY1-O3	82.52(11)
O5-DY1-O6	70.62(10)
O3-DY1-O6	141.43(11)
O5-DY1-O1	142.54(10)
O3-DY1-O1	78.54(10)
O6-DY1-O1	138.66(10)
O5-DY1-O4	81.89(12)
O3-DY1-O4	69.98(12)
O6-DY1-O4	79.03(12)
O1-DY1-O4	120.29(12)
O5-DY1-O7	149.07(10)
O3-DY1-O7	108.92(11)
O6-DY1-O7	84.18(10)
O1-DY1-O7	68.30(10)
O4-DY1-O7	75.79(11)
O5-DY1-O10	117.15(11)
O3-DY1-O10	144.78(10)
O6-DY1-O10	73.65(10)
O1-DY1-O10	68.30(10)
O4-DY1-O10	137.76(11)
O7-DY1-O10	69.99(10)
O5-DY1-O2	76.84(10)
O3-DY1-O2	83.22(10)
O6-DY1-O2	115.44(10)
O1-DY1-O2	69.10(10)
O4-DY1-O2	147.66(11)
O7-DY1-O2	131.87(10)
O10-DY1-O2	74.32(10)
O5-DY1-DY2	157.48(8)
O3-DY1-DY2	115.11(8)
O6-DY1-DY2	98.82(7)
O1-DY1-DY2	40.47(7)
O4-DY1-DY2	116.42(9)

O7-DY1-DY2	41.33(7)
O10-DY1-DY2	40.49(7)
O2-DY1-DY2	90.87(7)
O11-DY2-O12	70.91(11)
O11-DY2-O10	77.11(11)
O12-DY2-O10	121.79(11)
O11-DY2-O1	110.84(11)
O12-DY2-O1	78.04(10)
O10-DY2-O1	69.70(10)
O11-DY2-O9	83.46(11)
O12-DY2-O9	146.14(11)
O10-DY2-O9	70.91(11)
O1-DY2-O9	133.23(10)
O11-DY2-O7	146.07(11)
O12-DY2-O7	136.91(11)
O10-DY2-O7	70.93(10)
O1-DY2-O7	68.40(10)
O9-DY2-O7	75.70(11)
O11-DY2-O1M	80.78(12)
O12-DY2-O1M	77.99(11)
O10-DY2-O1M	142.09(11)
O1-DY2-O1M	147.88(11)
O9-DY2-O1M	76.33(11)
O7-DY2-O1M	118.73(10)
O11-DY2-O8	144.88(11)
O12-DY2-O8	80.20(11)
O10-DY2-O8	136.76(10)
O1-DY2-O8	81.21(10)
O9-DY2-O8	112.88(11)
O7-DY2-O8	68.91(10)
O1M-DY2-O8	73.89(12)
O11-DY2-DY1	115.24(8)
O12-DY2-DY1	118.10(8)
O10-DY2-DY1	41.88(7)
O1-DY2-DY1	40.84(7)
O9-DY2-DY1	92.45(8)
O7-DY2-DY1	41.10(7)
O1M-DY2-DY1	159.64(8)

Table S5. Geometry (Å, °) of the strong hydrogen-bonding motifs in compound **1**•MeOH

$D-H\cdots A$	$D-H$	$H\cdots A$	$D\cdots A$	$D-H\cdots A$
O1M-H1M \cdots O2M ⁱ	0.82(6)	1.88(6)	2.681(5)	163(5)
O2M-H2M \cdots O3	0.85(5)	1.88(5)	2.727(5)	176(6)

Symmetry codes: (i) 1+x, y, z.

Table S6. Bond lengths [Å] for **Y@Dy2** at 107.7(6) K with estimated standard deviations in parentheses.

Distance	Value
Y1-O5	2.254(3)
Y1-O3	2.286(3)
Y1-O6	2.313(3)
Y1-O10	2.390(3)
Y1-O1	2.354(3)
Y1-O4	2.343(3)
Y1-O7	2.331(3)
Y1-O2	2.427(3)
Y1-DY2	3.490(7)
Y1-Y2	3.549(1)
DY1-O5	2.199(9)
DY1-O6	2.401(11)
DY1-O7	2.461(7)
DY1-O2	2.266(8)
DY1-O3	2.237(14)
DY1-O10	2.388(12)
DY1-O1	2.313(9)

DY1-O4	2.460(10)
DY1-DY2	3.526(10)
DY1-Y2	3.585(9)
Y2-O11	2.248(3)
Y2-O12	2.284(3)
Y2-O7	2.383(3)
Y2-O1	2.330(2)
Y2-O8	2.414(3)
Y2-O1M	2.369(3)
Y2-O10	2.315(3)
Y2-O9	2.329(3)
DY2-O1	2.163(10)
DY2-O12	2.202(9)
DY2-O10	2.450(9)
DY2-O9	2.536(10)
DY2-O7	2.291(9)
DY2-O11	2.466(10)
DY2-O8	2.180(10)
DY2-O1M	2.434(9)

Table S7. Selected Bond angles [°] for **Dy@Y2** at 107.7(6) K with estimated standard deviations in parentheses.

Distance	Value
O5-Y1-O3	81.90(10)
O5-Y1-O6	70.99(10)
O3-Y1-O6	141.47(11)
O5-Y1-O10	116.84(11)
O3-Y1-O10	144.31(10)
O6-Y1-O10	73.93(10)
O5-Y1-O1	141.66(10)
O3-Y1-O1	78.64(10)
O6-Y1-O1	138.75(10)
O10-Y1-O1	68.06(9)
O5-Y1-O4	81.81(11)
O3-Y1-O4	70.29(11)
O6-Y1-O4	78.99(11)
O10-Y1-O4	138.61(10)
O1-Y1-O4	121.01(11)

O5-Y1-O7	149.97(10)
O3-Y1-O7	109.25(11)
O6-Y1-O7	84.63(9)
O10-Y1-O7	70.48(9)
O1-Y1-O7	68.30(9)
O4-Y1-O7	76.40(10)
O5-Y1-O2	76.03(9)
O3-Y1-O2	82.83(9)
O6-Y1-O2	115.07(11)
O10-Y1-O2	73.78(9)
O1-Y1-O2	69.02(9)
O4-Y1-O2	147.25(10)
O7-Y1-O2	131.85(10)
O5-Y1-DY2	160.76(17)
O3-Y1-DY2	111.29(18)
O6-Y1-DY2	102.47(19)
O10-Y1-DY2	44.55(17)
O1-Y1-DY2	37.46(17)
O4-Y1-DY2	115.32(19)
O2-Y1-DY2	91.35(18)
O7-Y1-DY2	40.53(19)
O2-Y1-Y2	90.51(7)
O5-Y1-Y2	156.85(10)
O3-Y1-Y2	115.50(8)
O6-Y1-Y2	98.92(7)
O10-Y1-Y2	40.26(6)
O1-Y1-Y2	40.48(6)
O4-Y1-Y2	117.50(8)
O7-Y1-Y2	41.71(7)
O5-DY1-O6	70.2(3)
O5-DY1-O7	143.6(4)
O6-DY1-O7	80.0(3)
O5-DY1-O2	80.5(3)
O6-DY1-O2	117.9(5)
O7-DY1-O2	133.5(4)
O5-DY1-O3	84.2(4)
O6-DY1-O3	138.7(4)
O7-DY1-O3	106.4(5)

O2-DY1-O3	87.7(3)
O5-DY1-O10	119.1(6)
O6-DY1-O10	72.4(4)
O7-DY1-O10	68.3(3)
O2-DY1-O10	76.8(3)
O3-DY1-O10	148.5(4)
O5-DY1-O1	149.4(4)
O6-DY1-O1	135.8(5)
O7-DY1-O1	66.8(2)
O2-DY1-O1	72.5(2)
O3-DY1-O1	80.5(4)
O10-DY1-O1	68.8(3)
O5-DY1-O4	80.3(3)
O6-DY1-O4	75.0(2)
O7-DY1-O4	71.9(2)
O2-DY1-O4	151.0(5)
O3-DY1-O4	68.9(4)
O10-DY1-O4	131.9(3)
O1-DY1-O4	117.8(5)
O5-DY1-DY2	163.1(6)
O6-DY1-DY2	99.6(3)
O7-DY1-DY2	40.3(2)
O2-DY1-DY2	93.2(4)
O3-DY1-DY2	111.4(4)
O10-DY1-DY2	43.9(2)
O1-DY1-DY2	36.5(3)
O4-DY1-DY2	110.8(4)
O5-DY1-Y2	158.7(6)
O6-DY1-Y2	96.2(3)
O7-DY1-Y2	41.43(15)
O2-DY1-Y2	92.3(3)
O3-DY1-Y2	115.7(4)
O10-DY1-Y2	39.61(14)
O1-DY1-Y2	39.62(15)
O4-DY1-Y2	112.9(3)
O11-Y2-O12	71.22(10)
O11-Y2-O7	146.58(10)
O12-Y2-O7	135.90(10)

O11-Y2-O1	110.93(10)
O12-Y2-O1	77.82(9)
O7-Y2-O1	67.84(9)
O11-Y2-O8	144.61(10)
O12-Y2-O8	79.40(10)
O7-Y2-O8	68.73(9)
O1-Y2-O8	80.68(9)
O11-Y2-O1M	80.97(10)
O12-Y2-O1M	77.71(10)
O7-Y2-O1M	118.95(10)
O1-Y2-O1M	147.29(11)
O8-Y2-O1M	73.76(10)
O11-Y2-O10	77.47(10)
O12-Y2-O10	122.16(10)
O7-Y2-O10	70.87(9)
O1-Y2-O10	69.73(9)
O8-Y2-O10	136.52(9)
O1M-Y2-O10	142.68(11)
O11-Y2-O9	84.43(11)
O12-Y2-O9	146.71(10)
O7-Y2-O9	75.82(10)
O1-Y2-O9	133.49(9)
O8-Y2-O9	112.35(10)
O1M-Y2-O9	76.29(10)
O10-Y2-O9	71.63(9)
O11-Y2-Y1	115.59(8)
O12-Y2-Y1	118.13(7)
O7-Y2-Y1	40.61(6)
O1-Y2-Y1	41.00(6)
O8-Y2-Y1	95.31(7)
O1M-Y2-Y1	159.39(8)
O10-Y2-Y1	41.85(7)
O9-Y2-Y1	92.52(7)
O11-Y2-DY1	113.75(18)
O12-Y2-DY1	116.02(17)
O7-Y2-DY1	43.12(14)
O1-Y2-DY1	39.29(19)
O8-Y2-DY1	96.5(2)

O1M-Y2-DY1	161.97(14)
O10-Y2-DY1	41.1(2)
O9-Y2-DY1	94.20(19)
O1-DY2-O12	83.2(4)
O1-DY2-O10	70.0(3)
O12-DY2-O10	119.8(5)
O1-DY2-O9	131.1(3)
O12-DY2-O9	137.7(4)
O10-DY2-O9	66.0(2)
O1-DY2-O7	72.3(2)
O12-DY2-O7	148.7(5)
O10-DY2-O7	70.1(2)
O9-DY2-O7	73.5(3)
O1-DY2-O11	108.9(4)
O12-DY2-O11	68.6(3)
O10-DY2-O11	71.0(3)
O9-DY2-O11	75.9(3)
O7-DY2-O11	137.6(4)
O1-DY2-O8	90.0(4)
O12-DY2-O8	86.5(3)
O10-DY2-O8	143.1(4)
O9-DY2-O8	113.1(5)
O7-DY2-O8	74.5(3)
O11-DY2-O8	145.8(3)
O1-DY2-O1M	157.4(4)
O12-DY2-O1M	77.9(2)
O10-DY2-O1M	130.7(4)
O9-DY2-O1M	71.4(3)
O7-DY2-O1M	120.0(5)
O11-DY2-O1M	75.5(3)
O8-DY2-O1M	76.7(3)
O1-DY2-Y1	41.45(14)
O12-DY2-Y1	123.2(4)
O10-DY2-Y1	43.19(13)
O9-DY2-Y1	90.4(2)
O7-DY2-Y1	41.39(14)
O11-DY2-Y1	111.4(3)
O8-DY2-Y1	101.7(3)

O1M-DY2-Y1	158.8(4)
O1-DY2-DY1	39.5(2)
O12-DY2-DY1	120.9(3)
O10-DY2-DY1	42.5(3)
O9-DY2-DY1	92.0(3)
O7-DY2-DY1	43.98(18)
O11-DY2-DY1	109.8(5)
O8-DY2-DY1	102.9(4)
O1M-DY2-DY1	161.2(3)
DY2-O1-Y1	101.1(2)
Y2-O1-Y1	98.52(9)
DY2-O1-DY1	103.9(4)
Y2-O1-DY1	101.1(3)
DY1-O7-Y2	95.5(2)
DY1-O7-DY2	95.7(3)
Y2-O7-Y1	97.68(9)
DY2-O7-Y1	98.1(3)
DY2-O10-Y1	92.3(2)
Y1-O10-Y2	97.88(10)
DY2-O10-DY1	93.6(3)
Y2-O10-DY1	99.3(3)

Table S8. Parameters obtained by fitting the Cole-Cole plots (1500 dc field, Figure 3e) of 1:MeOH using the sum of two generalized Debye functions.

T	$\Delta\chi_1$	$\Delta\chi_2$	α_1	α_2	τ_1	τ_2
1.8	3.33313	6.609	0.11239	0.48806	0.08699	0.00183
1.9	3.20179	6.66823	0.14812	0.50379	0.0789	0.0018
2	2.93556	6.66126	0.15095	0.50456	0.07479	0.00185
2.5	2.21439	5.82446	0.1884	0.47805	0.04587	0.00164
3	1.81643	4.9345	0.21725	0.45188	0.02688	0.00132
3.5	1.82428	3.82966	0.24748	0.40776	0.01508	8.84003E-4
4	1.76695	3.04706	0.24002	0.37069	0.00921	6.02288E-4
4.5	1.51216	2.5898	0.21808	0.33713	0.00665	4.88965E-4
5	1.35823	2.18504	0.21401	0.31361	0.00475	3.90499E-4
6	0.90384	1.6648	0.14422	0.23779	0.00333	3.26681E-4
7	0.61128	1.28968	0.10199	0.19307	0.00237	2.78417E-4
8	0.41084	0.94096	0.03841	0.11414	0.00187	2.62749E-4
9	0.28782	0.68026	0.02576	0.06072	0.00142	2.48878E-4
10	0.22378	0.48196	0.01827	0	0.00105	2.25511E-4

Table S9. Parameters obtained by fitting the out-of-phase (Figure 5b) versus T ac magnetic susceptibility signals for **Dy@Y2** in a 3.0 G ac field oscillating between 1488 and 10 Hz using the sum of two generalized Debye functions.

T	α_1	α_2	τ_1	τ_2 (fixed) taken from Tab. S7
1.8	0.50666	0.47611	0.12037	0.00183
1.9	0.52619	0.47155	0.12157	0.0018
2	0.548	0.48988	0.1174	0.00185
2.5	0.56303	0.49591	0.0973	0.00164
3	0.53468	0.46686	0.07734	0.00132
3.5	0.54144	0.47294	0.04837	8.84003E-4
4	0.52138	0.37567	0.02837	6.02288E-4
4.5	0.51715	0.3994	0.02073	4.88965E-4
5	0.49233	0.41928	0.01481	3.90499E-4
6	0.46589	0.40545	0.00803	3.26681E-4
7	0.41853	0.35795	0.0061	2.78417E-4
8	0.38227	0.30308	0.0041	2.62749E-4
9	0.40699	0.26806	0.0027	2.48878E-4

Table S10. Ab Initio CASSCF/RASSI-SO calculations of the energy barrier of the lowest 8 KD of both Dy centers in 1·MeOH along with the deviation in the angle of the excited state anisotropic axis with respect to the ground state.

KD	Dy-1(cm ⁻¹)	Angle(°)	Dy-2(cm ⁻¹)	Angle	Dy-1 <i>g_{xx}/g_{yy}/g_{zz}</i>	Dy-2 <i>g_{xx}/g_{yy}/g_{zz}</i>
1	0	0	0	0	0.387/2.827/14.944	0.009/0.022/19.688
2	14.00	87.4	120.47	15.7	0.542/2.253/14.907	0.702/1.591/15.910
3	42.40	27.2	168.88	73.6	1.764/3.015/14.254	2.482/3.313/13.451
4	80.89	40.6	227.75	115.1	2.486/5.517/12.962	7.416/6.259/2.518
5	126.04	86.4	286.85	84.9	1.720/4.467/10.367	1.574/2.679/11.096
6	176.21	114.1	316.75	83.5	1.567/2.110/15.847	0.749/1.035/15.450
7	278.48	89.2	377.73	74.5	0.061/0.080/19.802	0.169/0.419/18.719
8	523.36	131.6	695.87	119.9	0.004/0.009/19.923	0.001/0.002/19.913

Table S11. *Ab initio* computed crystal field parameters for Dy-1 and Dy-2 centres of 1-MeOH

Dy-1			Dy-2		
k	q	B(k,q)	k	q	B(k,q)
2	-2	-5.23E+00	2	-2	7.00E+00
	-1	8.99E+00		-1	-1.12E+01
	0	2.85E+00		0	-3.28E+00
	1	-4.98E+00		1	-8.78E+00
	2	-2.24E-01		2	-1.94E+00
4	-4	-3.66E-02	4	-4	-5.15E-03
	-3	1.34E-02		-3	-4.31E-01
	-2	-2.15E-02		-2	1.34E-01
	-1	2.58E-01		-1	-5.97E-02
	0	4.21E-02		0	-3.81E-02
	1	-7.04E-02		1	-5.44E-02
	2	8.44E-03		2	-3.87E-03
	3	1.48E-01		3	3.73E-01
	4	-3.50E-02		4	-1.54E-02
6	-6	-1.96E-03	6	-6	-2.34E-03
	-5	5.33E-03		-5	1.32E-02
	-4	-1.06E-03		-4	-9.31E-04
	-3	-3.80E-03		-3	-4.91E-03
	-2	-4.22E-03		-2	-1.83E-03
	-1	6.65E-03		-1	4.05E-03
	0	2.33E-04		0	1.23E-04
	1	-3.34E-04		1	3.90E-03
	2	-1.05E-03		2	-3.54E-03
	3	9.74E-04		3	4.98E-03
	4	4.09E-03		4	-3.79E-03
	5	-6.78E-03		5	6.70E-03
	6	-1.68E-03		6	4.10E-03

The following Hamiltonian is used for calculating the crystal field parameters.

$$H_{CF} = \sum_{k,q} B_k^q O_k^q$$

Where $O_k^q =$ extended Stevens operator

k=rank of ITO=2,4,6

q=component of the ITO=-k,-k+1,.....,0,.....,k

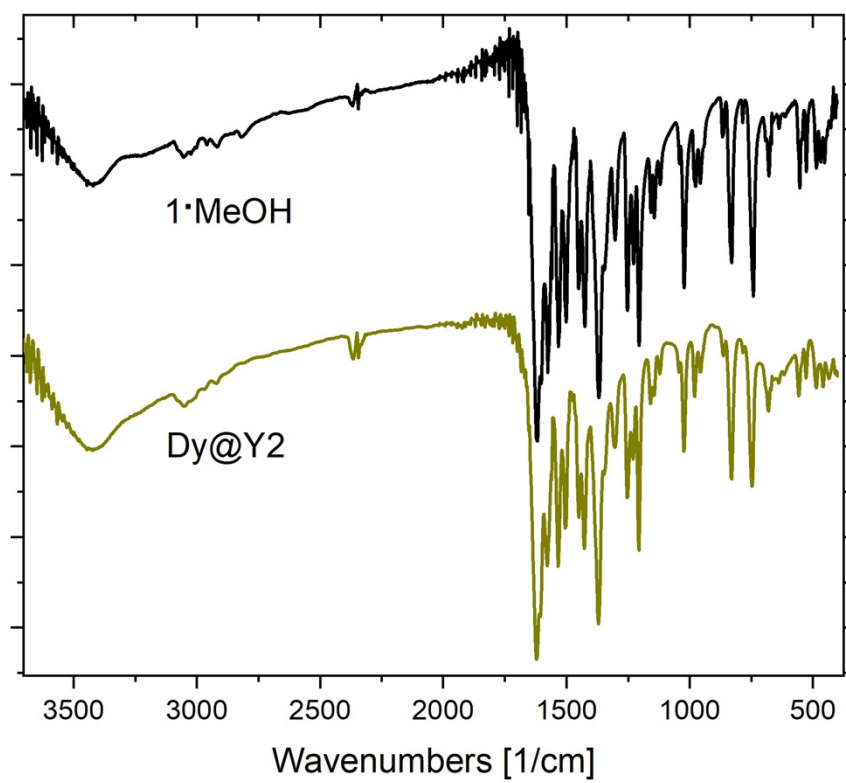


Figure S 1. The IR spectra (KBr, cm⁻¹) of **1·MeOH** and **Dy@Y2**.

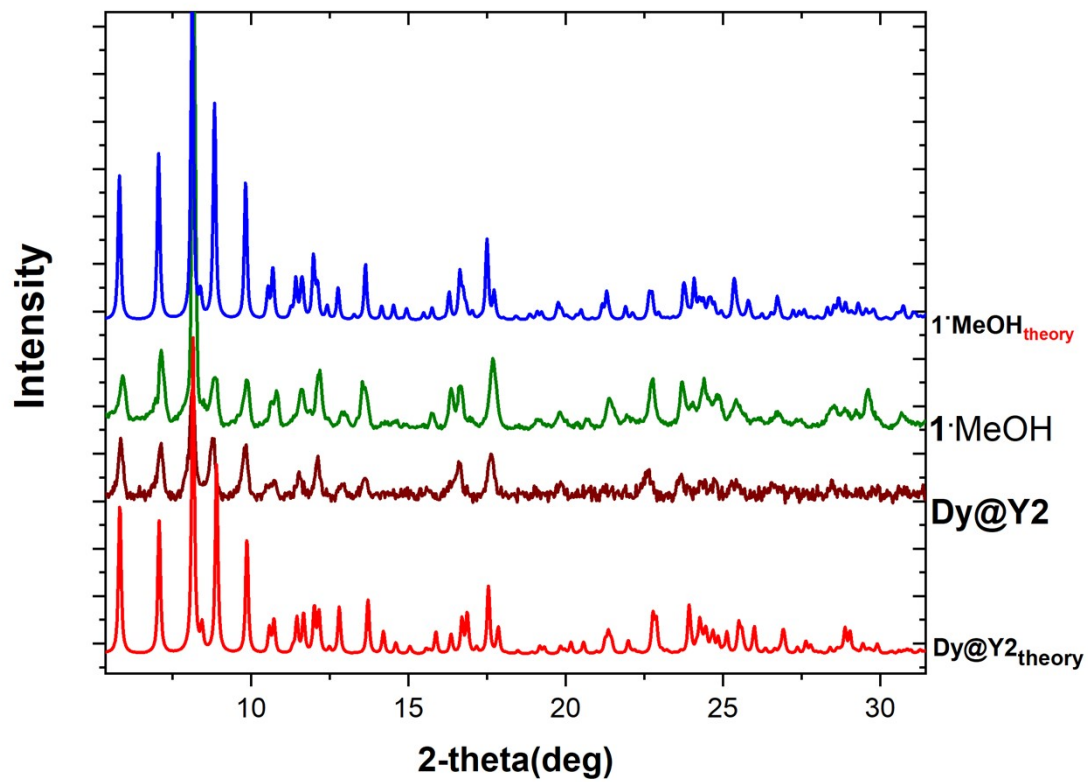


Figure S 2. Experimental and theoretical X-ray powder patterns of $1:MeOH$ and $Dy@Y2$.

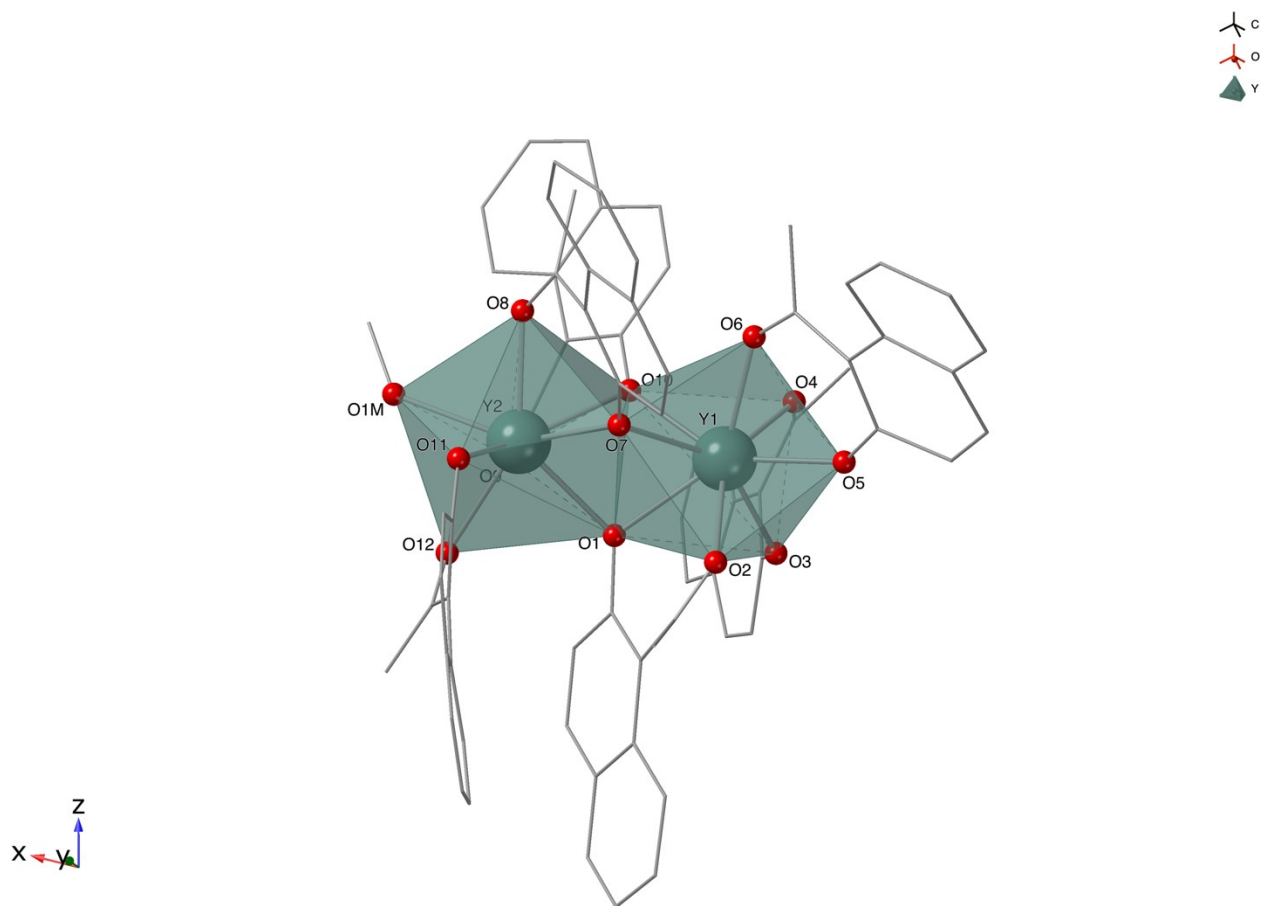


Figure S 3. Partially labelled plot of the crystal structure of **Dy@Y₂**. The polyhedral representations of the Y^{III} atoms are also shown. Hydrogen atoms and the dopant Dy^{III} ions have been omitted for the sake of clarity.

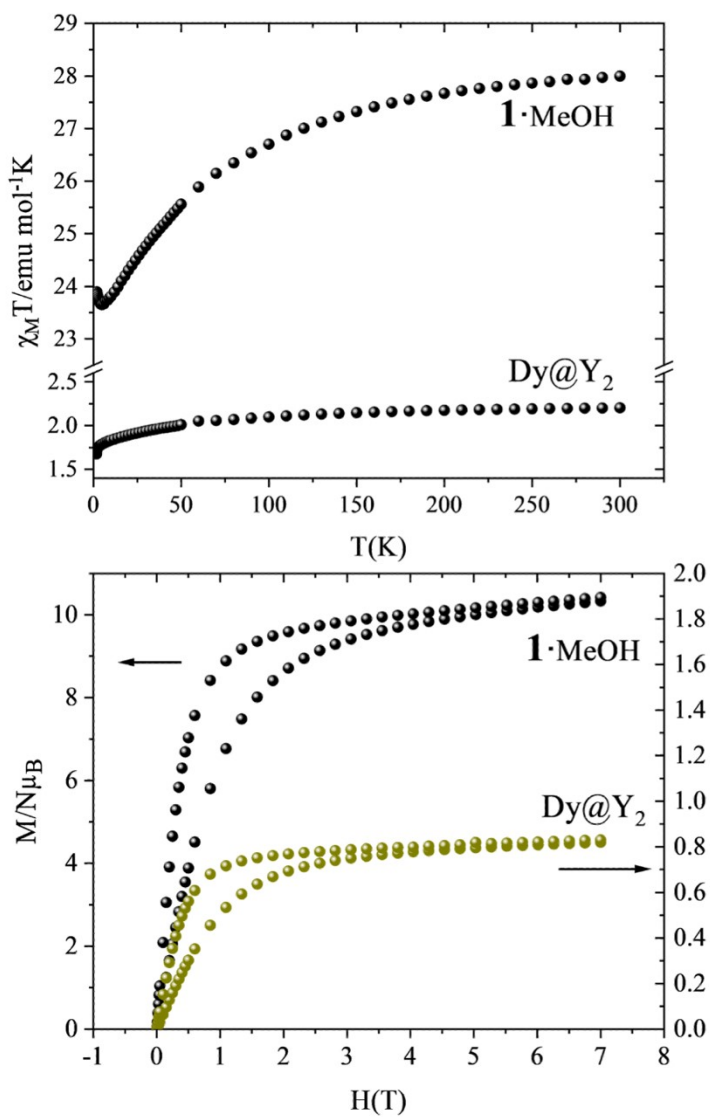


Figure S 4. (upper) Dc magnetic susceptibility of of $1 \cdot \text{MeOH}$ and Dy@Y_2 in the 300-2 K temperature range under an applied field of 0.1 T. (lower) Isothermal magnetization curves of $1 \cdot \text{MeOH}$ and Dy@Y_2 at 2K and 5K.

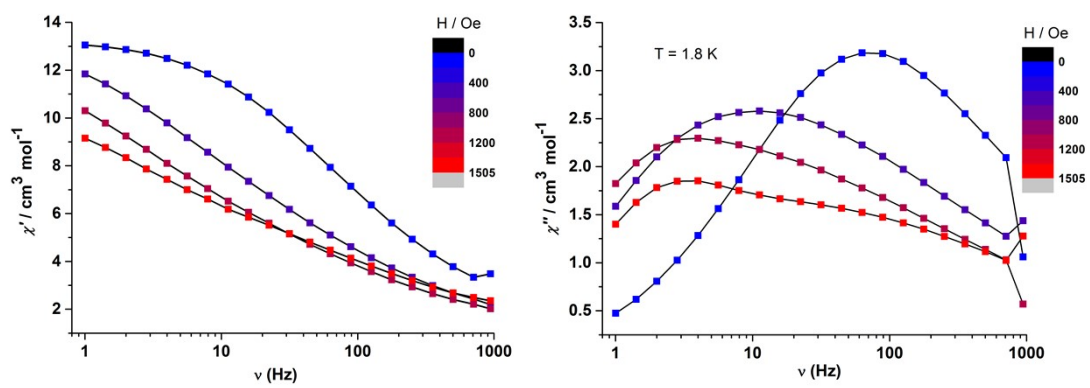


Figure S 5. Field dependence of the out-of-phase ac susceptibility signals for **1-MeOH**

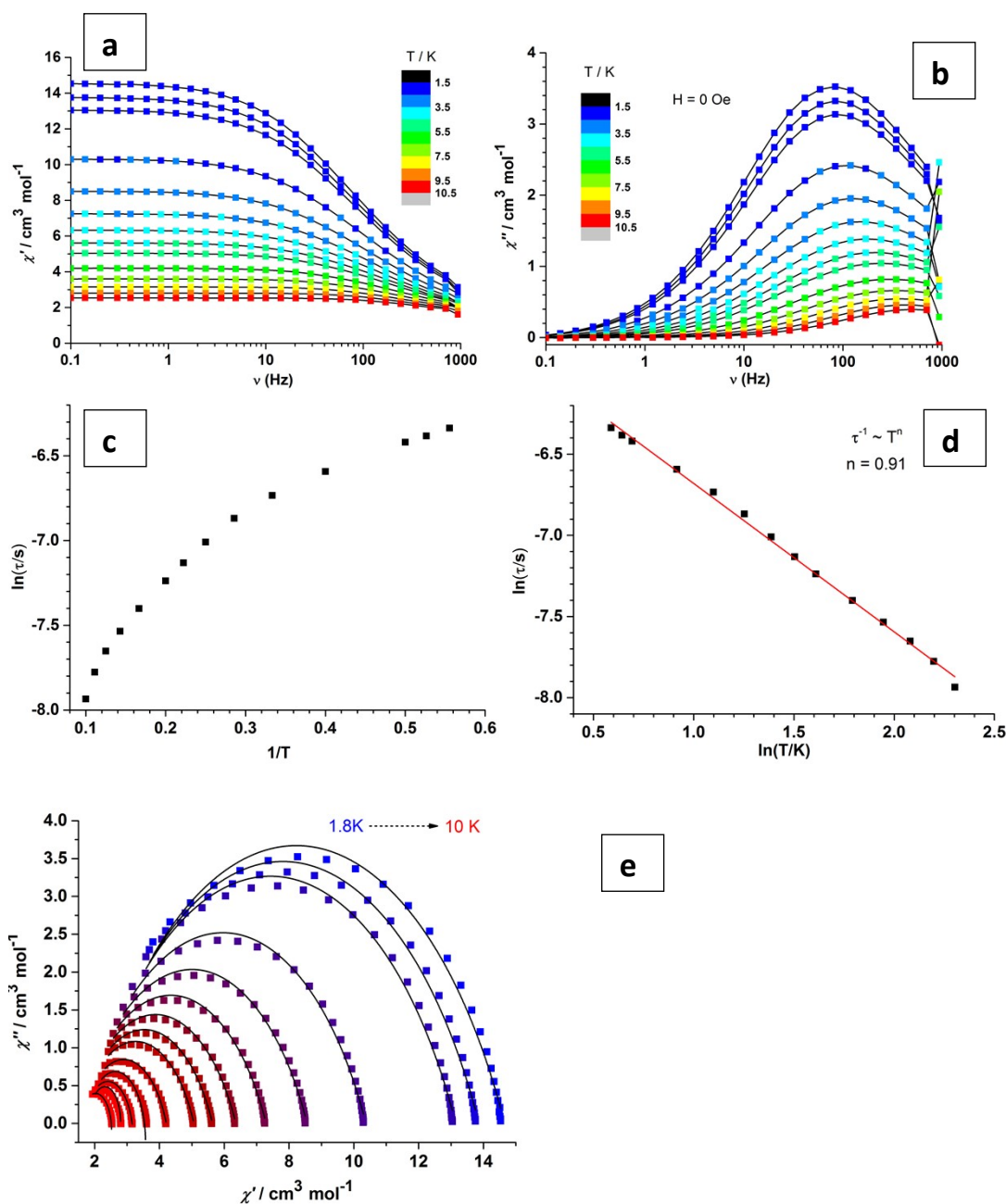


Figure S 6. (a)-(b) The weak temperature dependent χ'' signals were observed under zero dc field, indicating a small effective barrier. (c)-(d) No linear region is observed in Arrhenius fitting, while an exponential (T^n) fitting gives n value close to 1, suggesting the direct relaxation process present here. (e) The fitting of Cole-Cole plots with a generalized Debye model gives α values between 0.12 and 0.34. All curves are refer to 1:MeOH

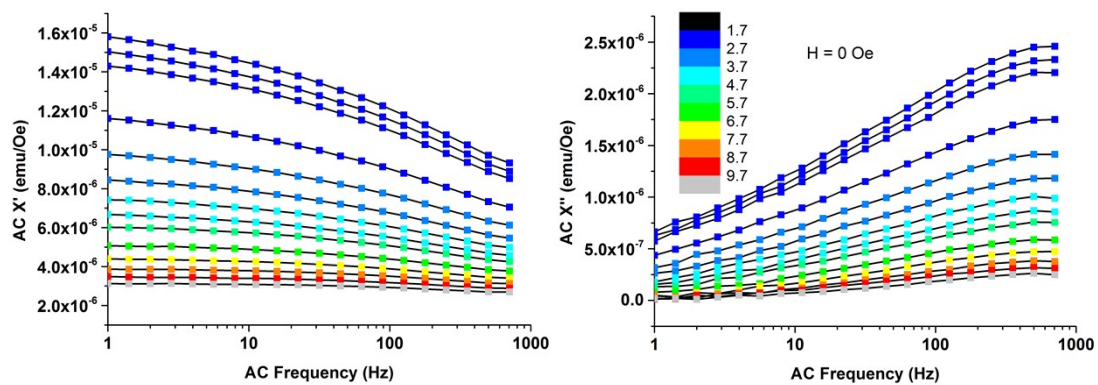


Figure S 7. Under zero field, no χ_M'' peaks were observed for the sample **Dy@Y2**

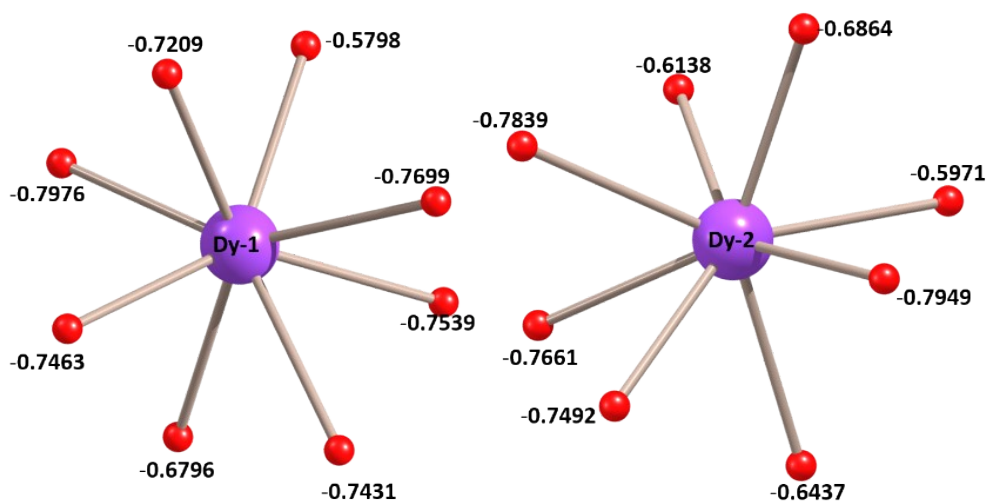


Figure S 8. LoProp charge on the surrounding O of both Dy-1 and Dy-2 centres of **1·MeOH**

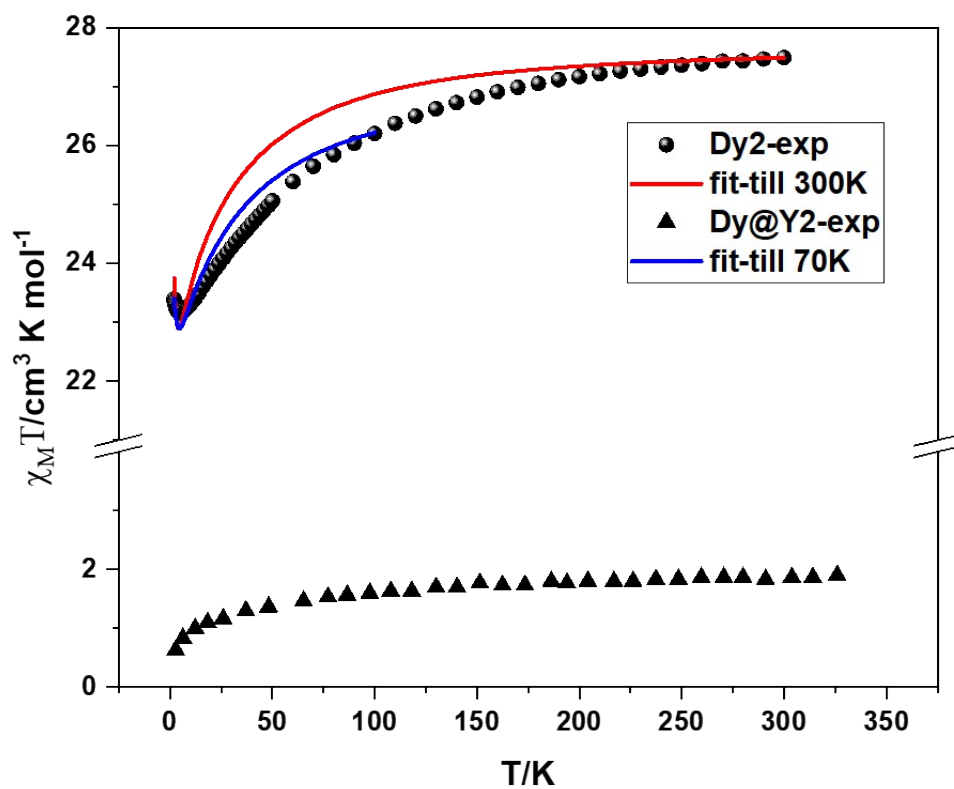


Figure S 9. Poly_aniso fitted magnetic susceptibility for sample 1·MeOH (solid spheres). The magnetic susceptibility of **Dy@Y2** (solid triangles) is also presented for comparison reasons

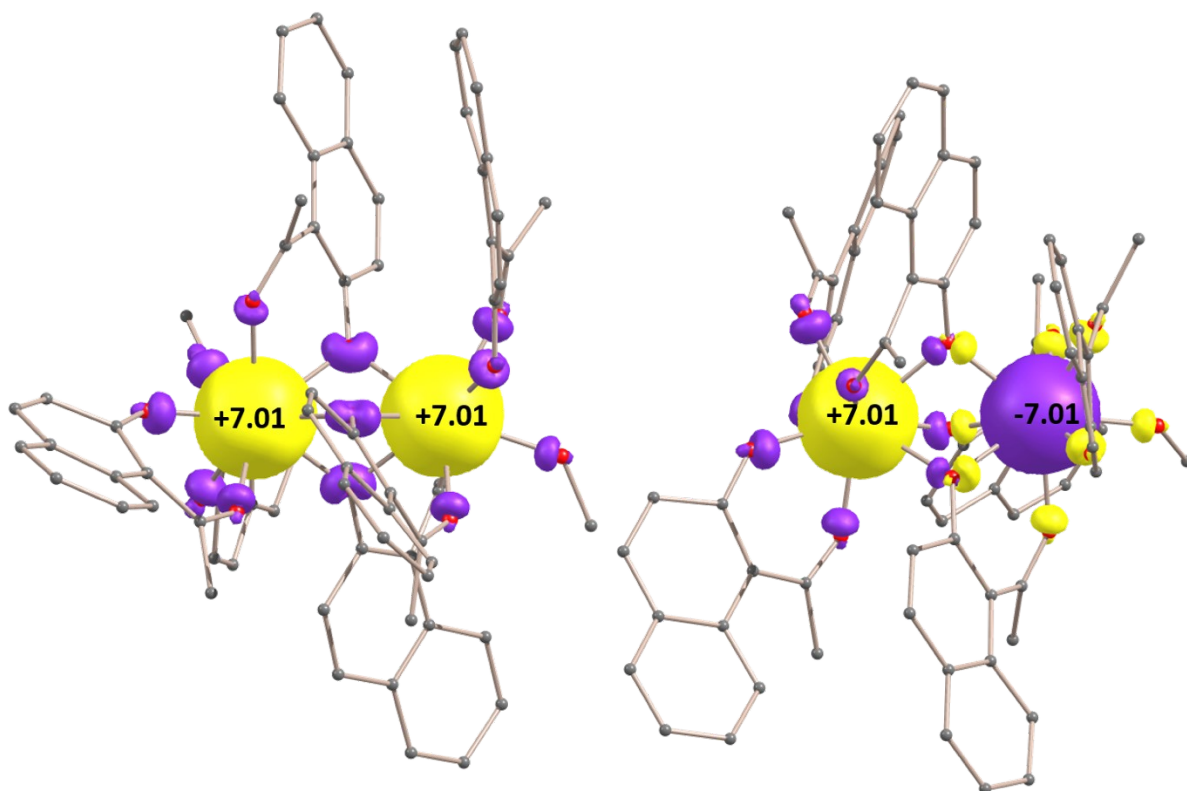


Figure S 10. Spin density plots for the high spin and broken symmetry states, obtained from the density function calculations using broken symmetry approach for **1**·MeOH

The exchange has been calculated using the following equation,

$$J_{exch} = \frac{E_{BS} - E_{HS}}{2S_1S_2 + S_2}$$

E_{BS} = energy of broken symmetry state, E_{HS} = Energy of high spin state